Volume 1 | Number 1 | Jan 2013 | Pages 1–100

ChemComm

Chemical Communications
www.rsc.org/chemcomm

ROYAL SOCIETY
OF CHEMISTRY

This is an *Accepted Manuscript*, which has been through the Royal Society of Chemistry peer review process and has been accepted for publication.

Accepted Manuscripts are published online shortly after acceptance, before technical editing, formatting and proof reading. Using this free service, authors can make their results available to the community, in citable form, before we publish the edited article. We will replace this *Accepted Manuscript* with the edited and formatted *Advance Article* as soon as it is available.

You can find more information about *Accepted Manuscripts* in the **Information for Authors**.

Please note that technical editing may introduce minor changes to the text and/or graphics, which may alter content. The journal's standard **Terms & Conditions** and the **Ethical guidelines** still apply. In no event shall the Royal Society of Chemistry be held responsible for any errors or omissions in this *Accepted Manuscript* or any consequences arising from the use of any information it contains.

www.rsc.org/chemcomm

ChemComm

COMMUNICATION

Solution Phase Post-modification of Trimesic Acid Network on Au(111) with Zn^{2+} Ions†

Jaesung Lee[a], Jandee Kim[a], Hyeran Kim[b], Choong Kyun Rhee*,[a], Myung-Hwan Whangbo[c]

Solution phase post-modification of trimesic acid (TMA) network on Au(111) with Zn^{2+} ions was found to induce a transformation of a bar-featured scanning tunneling microscopy image of ($5\sqrt{3} \times 5\sqrt{3}$) to a chevron-pair image of ($10\sqrt{3} \times 10\sqrt{3}$). Voltammetric determination of Zn coverage in the modified TMA network support that the chevron feature consist of three TMA molecules combined via two coordination bonds between Zn^{2+} ions and carboxylates of the TMAs.

Two dimensional architecture of metal-organic coordination monolayers on solid surfaces has drawn much attention from the viewpoints of fundamental sciences and practical applications.[1-7] The metal-organic coordination networks[8] utilize the coordination between transition metals and organic ligands, which is stronger than other non-covalent bonds such as hydrogen bond and van der Waals interaction. The diverse directional bonds provided by coordination chemistry are anticipated to provide useful properties such as nanostructured templates, molecular magnetism, and heterogeneous catalysis.[9] The properties of metal-organic coordination monolayers are determined by several factors. The structures depend strongly on the metal-to-ligand ratio as exemplified by the structures of Fe/terephthalic acid (1,4-dicarboxylic benzoic acid), which change from a cloverleaf phase to a ladder phase to a single-row phase as the relative amount of Fe increases.[10,11] The length of organic ligands determines pore sizes,[12-14] and the chiral interactions between metals and ligands govern the chirality of resulting networks.[15-17] On the other hand, the substrate surfaces are well known to play a significant role in forming metal-organic coordination monolayers.[13,18] In most studies on metal-organic coordination monolayers, they examine the layers prepared under ultrahigh vacuum (UHV) environments.[1] In this work we show that, when treated with a solution containing Zn^{2+} ions, a contoured network of anionic trimesic acid (TMA, 1,3,5-tricarboxylic benzoic acid) on Au(111) can be modified to form a metal-organic coordination monolayer. Our work suggests that the scope of promising applications can be widened by employing materials and methods not compatible to UHV.

Experimental details are described in ESI. Briefly, the formation of pristine TMA network was performed by contacting Au(111) with a solution of 1 mM TMA (95%, Aldrich) in 0.1 M $HClO_4$ (Suprapur, Aldrich) solution for 60 min.[19] A post-modification of the TMA network with Zn^{2+} ions was carried out by immersing the Au(111) crystal with a pristine TMA layer to a 0.1 M $HClO_4$ solution of 1 mM Zn acetate (99.99%, Merck) for more than 3 h. Electrochemical measurements were carried out in 0.1 M phosphate buffer solution (99.7% Aldrich) of pH 4.4 using a conventional three-electrode system with a Ag/AgCl electrode with 1.0 M NaCl solution.

The TMA adlayer formed on Au(111) in 0.1 M $HClO_4$ solution of 1 mM TMA is a nanoporous network of ($5\sqrt{3} \times 5\sqrt{3}$)R30°.[19] Details of the pristine TMA network are described in ESI. Briefly, the primary motif of the TMA network is a crown-like anionic TMA hexamer. The three carboxylic acid groups in each TMA molecule play different roles in weaving the network: one becomes a carboxylate group anchoring to the surface, another forms a hydrogen bond to the carboxylate group in the adjacent TMA molecule to complete a hexamer, and the other interconnects to the next TMA hexamers via hydrogen bonds to results in a network. Thus, the TMA adlayer is a contoured network of the crown-like anionic TMA hexamers.

Fig. 1 shows the STM images of a TMA network on Au(111) obtained in 0.1 M $HClO_4$ solution after a contact with a solution containing Zn^{2+} ions. In Fig. 1(a), three regions are recognizable: a domain of well-ordered STM spots (region I), that of partially ordered spots (region II), and an amorphous domain (region III). Fig. 1(b) shows a zoomed-in STM image of the region I, which consists of chevron pairs only. As indicated in the inset of Fig. 1(b), two different chevron pairs are distinguishable. One is a chevron pair whose opening is parallel to the [01] direction (denoted by black lines and referred hereafter to as the p-pairs), and the other is a chevron pair whose opening is rotated by 30° clockwise to the [2$\bar{1}$] direction (denoted by blue lines and referred hereafter to as the cw-pairs). The p- and cw-pairs queue along the arrows of the solid and dashed lines (parallel to the [2$\bar{1}$] direction), respectively, to form different chevron pair rows. Then, a sequential repetition of the p- and cw-pair rows along the [01] direction fills the ordered domain. The unit cell of this particular arrangement of the chevron pairs is a parallelogram depicted in Fig. 1(b): the length and interior angle are 4.88 ± 0.06 nm (equivalent to $10\sqrt{3}a_{Au}$) and ~120°, respectively. In addition, the unit cell is rotated by ~30° against the [01] direction so that the unit cell is assignable to a hexagonal ($10\sqrt{3} \times 10\sqrt{3}$)R30°, as schematically described in Fig. 1(c). On the other hand, there is
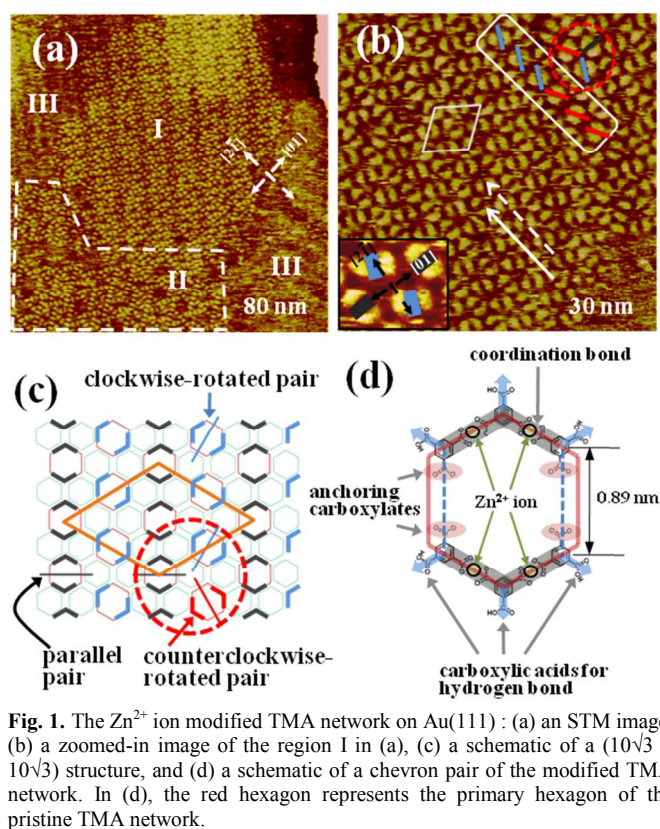
Fig. 1. The Zn^{2+} ion modified TMA network on Au(111) : (a) an STM image, (b) a zoomed-in image of the region I in (a), (c) a schematic of a ($10\sqrt{3} \times 10\sqrt{3}$) structure, and (d) a schematic of a chevron pair of the modified TMA network. In (d), the red hexagon represents the primary hexagon of the pristine TMA network.

another option in forming the chevron pairs rotated against the [$2\bar{1}$] direction. In the rectangle in Fig. 1(b), the chevron pairs (blue lines) are rotated clockwise, while the others (red lines) are counterclockwise. A situation under which the three different chevron pairs meet together as in the circle in Fig. 1(b) is demonstrated in the schematic diagram of Fig. 1(c). In the region II, there are chevron pairs arranged in a partially ordered manner. In particular, there are several recognizable short rows similar to that of the p-pairs in region I: their running directions are parallel to or rotated roughly by 60° from that in the region I. Among such regularly arrayed chevron pair queues, there are other chevron pairs scattered irregularly but rotated 30° in either direction against the running directions. Therefore, the region II is a domain in the middle of ordering. On the other hand, the regions III are totally amorphous with no discernible chevron pair, perhaps representing an incubational period of crystallization.

To account for the chevron pairs in the STM images of Fig. 1(a) and (b), we propose a primary motif depicted in Fig. 1(d). The wings of the chevron pairs are 0.79 ± 0.03 nm long, and the openings in chevron pairs are 0.89 ± 0.02 nm wide. The chevron pair is superimposable on the primary motif of the pristine TMA network, implying that the integrity of the TMA network was preserved. The distance between TMAs (0.79 nm) in chevron is certainly shorter than that in the bar features (0.83 nm) in the pristine TMA network. Because the Zn^{2+} ions modify the bar features in the ($5\sqrt{3} \times 5\sqrt{3}$) pattern to the chevron pairs in the ($10\sqrt{3} \times 10\sqrt{3}$) array, the most probable chemical bonding responsible for the chevron would be a strong metal-organic coordination bond between a Zn^{2+} ion and two carboxylates of two TMAs (Fig. 1(d)). From the model proposed for the chevron one can deduce the coverage of Zn^{2+} ions in the modified TMA network. Since each chevron pair has four Zn^{2+} ions (Fig. 1(d)), the coverage of Zn^{2+} ion in the ($10\sqrt{3} \times 10\sqrt{3}$) unit cell (Fig. 1(c)) is 0.053 (=16/300) (see ESI). Here, the coverage is

defined as the number ratio of Zn^{2+} ions to surface Au atoms within a unit cell.

For independent determination of the Zn^{2+} ion coverage, coulometry measurements of underpotential deposition (UPD) of Zn^{2+} ions on Au(111)[20,21] was utilized. The voltammograms of thin red and thick black lines in Fig. 2(a) were obtained on bare Au(111) in an 0.1 M phosphate buffer electrolyte (pH 4.4) without and with 1 mM Zn^{2+} ion, respectively. Without Zn^{2+} ions in the buffer solution only a redox couple of phosphate adsorption at ~0.2 V is discernible (In ESI a voltammogram of the employed Au(111) in 0.05 M H_2SO_4 is presented to firm its high quality.). In the presence of Zn^{2+} ions an additional redox peak representing UPD of Zn^{2+} ions on Au(111) appears at ~-0.35 V, accompanied with the shift of the hydrogen evolution onset potential from -0.55 V to -0.70 V and the preservation of the phosphate adsorption peak at ~0.2 V. Phosphate ions are well known to adsorb on UPD Zn layer on Au(111) to turn the whole UPD process to an one electron process (i.e., $Zn^{2+}(aq) + H_2PO_4^-(aq) + e^- \rightarrow Zn-H_2PO_4(ad)$). [21] Also, the coverage of UPD Zn on Au(111) was measured to be 0.33 using STM.[20] Therefore, the theoretical charge of Zn UPD in the presence of phosphate is ~74 $\mu C/cm^2$, and the measured charge in Fig. 2(a) (the hatched part) is ~70 $\mu C/cm^2$. Shown in Fig. 2(b) are the voltammograms of Au(111) covered with TMA networks before and after modification with Zn^{2+} ions (thin red and thick black lines, respectively) obtained in the Zn^{2+}-free phosphate buffer electrolyte. The unmodified TMA network on Au(111) induces a changes in the peak shape of phosphate adsorption. When modified with Zn^{2+} ions, an additional charge below -0.4 V appears accompanied with a potential shift of the phosphate adsorption peak. With continued voltammetric cycles,
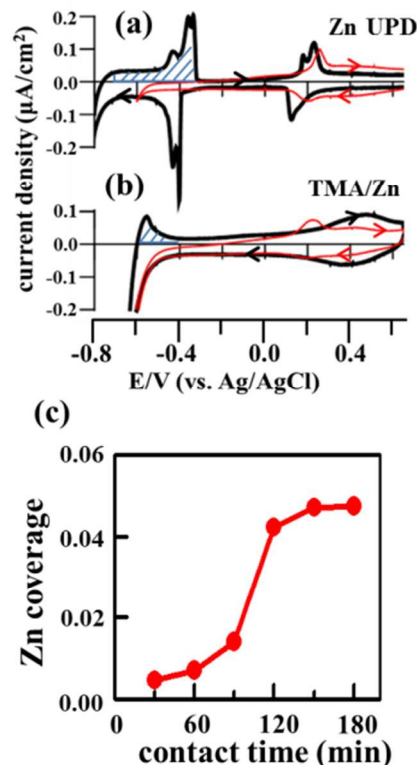

Fig. 2. (a) Cyclic voltammograms of bare Au(111) without and with 1 mM Zn^{2+} ion (thin red and thick black lines, respectively). (b) Cyclic voltammograms of Au(111) covered with TMA network before and after modification with Zn^{2+} ions (thin red and thick black lines, respectively). (c) A plot of Zn coverage as a function of contact time. Electrolyte: 0.1 M phosphate buffer (pH 4.4). Scan rate: 10 mV/sec.

however, the voltammogram of thick black line converges to that of thin red line, revealing that the species responsible for the additional charge below -0.4 V diffuses out from the surface without desorption of TMA. Therefore, the evolution in the voltammogram of the modified TMA network clearly demonstrates that the additional charge below -0.4 V (the hatched part of Fig. 2(b)) is due to UPD of Zn^{2+} ions in the modified TMA network, whose charge is ~13 $\mu C/cm^2$ (equivalent to the Zn coverage of 0.06). This particular value is comparable to the estimated coverage (0.056) of the proposed model (Fig. 1(d)). If each hydrogen bond in the pristine TMA network were to accommodate one Zn^{2+} ion, then the Zn^{2+} ion coverage would be 0.12, much larger than the experimentally determined value. Furthermore, the presence of Zn^{2+} ions in the modified TMA network causes a potential shift of the phosphate adsorption peak due probably to a difference in the modified and unmodified networks, while the amount of UPD Zn from the modified network may be too small to shift the hydrogen evolution potential as much as on bare Au(111).

Two more experimental observations should be addressed. One is a plot of electrochemically measured Zn coverage as a function of contact time between TMA network and Zn^{2+} ion-containing solution (Fig. 2(c)). The observed Zn coverage becomes nearly saturated after a contact for 120 min, revealing a slow chemical transformation to a modified network and a stoichiometric amount of Zn. If the interaction between the anionic TMA network and Zn^{2+} ion is simply electrostatic, the Zn coverage should not depend on the contact time (See below). The other is that the chevron-pair image of $(10\sqrt{3} \times 10\sqrt{3})$ at open-circuit potential (~-0.35 V) changes to an amorphous image at -0.6 V in the phosphate buffer after UPD of Zn^{2+} ions in the modified TMA network (Fig. 3). Certainly the electrochemical extraction of the Zn^{2+} ions from the modified TMA network of the $(10\sqrt{3} \times 10\sqrt{3})$ structure turns the remaining TMA adlayer amorphous. Namely, the presence of Zn^{2+} ions in TMA network is crucial in forming the $(10\sqrt{3} \times 10\sqrt{3})$ structure. Thus, during a contact between TMA network and Zn^{2+} ion-containing solution, Zn^{2+} ions are chemically incorporated into the pre-existing TMA network of $(5\sqrt{3} \times 5\sqrt{3})$ to slowly evolve to the metal-organic network of $(10\sqrt{3} \times 10\sqrt{3})$. Indeed, a simultaneous exposure of TMA and Zn^{2+} ions to Au(111) did not produce any ordered structure as
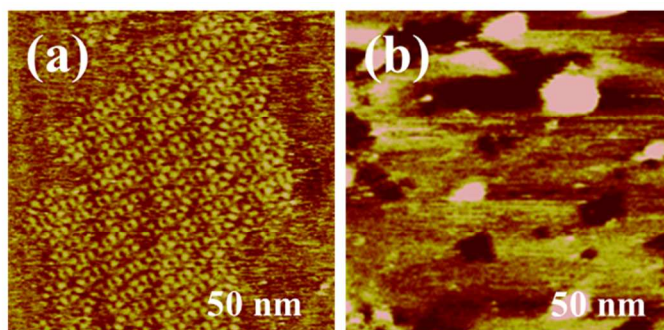
demonstrated in ESI, indicating that a post-modification of TMA network with Zn^{2+} ion is the only way to the metal-organic network of $(10\sqrt{3} \times 10\sqrt{3})$.

Fig. 3. STM images of Zn^{2+} modified TMA network on Au(111) at (a) open-circuit potential (~-0.35 V) and (b) -0.6 V for UPD of Zn in phosphate buffer.

The interaction between Zn^{2+} ions and TMA network would alter the adsorption configuration of TMAs, thus modifying the observed features in STM images. In the TMA network of $(5\sqrt{3} \times 5\sqrt{3})$, the bar feature of 0.83 nm long stands for two swiveled TMAs bound via a hydrogen bond.[19] Each chevron feature denotes three TMAs tied together by means of Zn^{2+}-carboxylate coordination bonds (Fig. 1(d)). The shorter length of chevron wing (0.79 nm) signals

movement of TMAs at the ends of a chevron to the central TMA, so that the openings in the chevron pairs (0.89 nm) become larger than the side length (0.83 nm) of the primary hexagon in the pristine TMA network. Most likely, the two carboxylates of the TMAs at the ends of a chevron anchor to the Au surface via carboxylate anion adsorption, and the remaining three carboxylic acids connect to the nearby three other chevrons via hydrogen bond (Fig. 1(d)).

The interaction between a TMA network on Au(111) and metal ions depends on contacting metal ion.[19] Zn^{2+} ions modify the TMA network due to coordination bond formation. On the other hand, Cu^{2+} ions selectively adsorb into the pores of the TMA hexamers due most likely to an electrostatic interaction between a Cu^{2+} ion and six carboxylates in a TMA hexamer including the interaction with Au surface. Indeed, the adsorption of Cu^{2+} ions into the pores was completed after a contact for 15 min. Depending on the stabilities of the two possible interactions (i.e., coordination bond and adsorption into anionic pores) one of them may be operational. More details need further work.

This work demonstrated for the first time a solution phase post-modification of the contoured network of anionic TMA on Au(111) with Zn^{2+} ion. A simple contact of a pristine TMA network with Zn^{2+} ions induced a transformation of a bar-featured STM image of $(5\sqrt{3} \times 5\sqrt{3})$ to a chevron-pair image of $(10\sqrt{3} \times 10\sqrt{3})$, proposed to be due to the formation of Zn^{2+}-carboxylate coordination bonds.

Notes and references

a Department of Chemistry, Chungnam National University, Daejeon 305-764, Korea. E-mail: ckrhee@cnu.ac.kr, nima89@naver.com, jdjd83@cnu.ac.kr; Fax: +82 42 821 8896; Tel: +82 42 821 5483

b Division of Materials Science, Korea Basic Science Institute, Daejeon 305-333, Korea. E-mail: khr2383@kbsi.re.kr; Fax: +82 42 865 3610; Tel: +82 42 865 3638

c Department of Chemistry, North Carolina State University, Raleigh, NC 27695, USA. E-mail: whangbo@ncsu.edu; Fax: +1 919 515 5079; Tel: +1 919 515 3464

1   F. Klappenberger, *Prog. Surf. Sci.*, 2014, **89**, 1.

2   H.-J. Gao, L. Gao, *Prog. Surf. Sci.*, 2010, **85**, 28.

3   H. Liang, Y. He, Y. Ye, X. Xu, F. Cheng, W. Sun, X. Shao, Y. Wang, J. Li, Kai Wu, *Coord. Chem. Rev.*, 2009, **253**, 2959.

4   J. A. A. W. Elemans, S. Lei, S. De Feyter, *Angew. Chem. Int. Ed.*, 2009, **48**, 7298.

5   N. Lin, S. Stepanow, M. Ruben, J.V. Barth, , Top. Curr. Chem., 2009, **287**, 1.

6   S. Furukawa, S. De Feyter, *Top. Curr. Chem.*, 2009, **287**, 87.

7   F.S. Tautz, *Prog. Surf. Sci.*, 2007, **82**, 479.

8   A. Dmitriev, H. Spillmann, N. Lin, J.V. Barth, K. Kern, *Angew. Chem. Int. Ed.*, 2003, **42**, 2670.

9   J.V. Barth, *Surf. Sci.*, 2009, **603**, 1533.

10   A. Dmitriev, H. Spillmann, N. Lin, J. V. Barth, K. Kern, *Angew. Chem. Int. Ed.*, 2003, **115**, 2774.

11   M. A. Lingenfelder, H. Spillmann, A. Dmitriev, S. Stepanow, N. Lin, J. V. Barth, K. Kern, *Chem. Eur. J.*, 2004, **10**, 1913.

12 A. Langner,; S. L. Tait, N. Lin, C. Rajadurai, M. Ruben, K. Kern, *PNAS*, 2007, **104**, 17927.

13 S. Stepanow, N. Lin, J. V. Barth, K. Kern, *J. Phys. Chem. B*, 2006, **110**, 23472.

14 U. Schlickum, R. Decker, F. Klappenberger, G. Zoppellaro, S. Klyatskaya, M. Ruben, I. Silanes, A. Arnau, K. Kern, H. Brune, J. V. Barth, *Nano Lett.*, 2007, **7**, 3813.

15 S. Stepanow, N. Lin, D. Payer, U. Schlickum, F. Klappenberger, G. Zoppellaro, M. Ruben, H. Brune, J. V. Barth, K. Kern, *Angew. Chem. Int. Ed.*, 2007, **119**, 724.

16 P. Messina, A. Dmitriev, N. Lin, H. Spillmann, M. Abel, J. V. Barth, Kern, K. *J. Am. Chem. Soc.*, 2002, **124**, 14000.

17 H. Spillmann, A. Dmitriev, N. Lin, P. Messina, J. V. Barth, K. Kern, *J. Am. Chem. Soc.*, 2003, **125**, 10725.

18 N. Lin, A. Langner, S. L. Tait, C. Rajadurai, M. Ruben, K. Kern, *Chem. Commun.*, 2007, 4860.

19 J. Kim, C. K. Rhee, H.-J. Koo, E. E. Kasapbasi, M.-H. Whangbo, *J. Phys. Chem. C*, 2013*, **117***, 22636.

20 S. Takahashi, A. Aramata, M. Nakamura, K. Hasebec, M. Taniguchi, S. Taguchi, A. Yamagish, *Surf. Sci.*, 2002, **512**, 37.

21 A. Aramataa, S. Taguchi, T. Fukuda, M. Nakamura, G. Horanyi, *Electrochim. Acta*, 1998, **44**, 999.